Supplementary Material

Integration of neutron time-of-flight single-crystal Bragg peaks in reciprocal space

Arthur J. Schultz[a]*, Mads Ry Vogel Jørgensen[b], Xiaoping Wang[c]*, Ruth L. Mikkelson[d], Dennis J. Mikkelson[d], Vickie E. Lynch[e], Peter F. Peterson[e], Mark L. Green[f] and Christina M. Hoffmann[c]*

[a]X-Ray Science Division, Argonne National Laboratory, Argonne, Illinois, 60439, USA, [b]Center for Materials Crystallography, Aarhus University, Aarhus, Denmark, [c]Chemical and Engineering Materials Division, Oak Ridge National Laboratory, Oak Ridge, Tennessee, 37831, USA, [d]Department of Mathematics, Statistics and Computer Science, University of Wisonsin-Stout, Menomonie, Wisconsin, 54751, USA, [e]Neutron Data Analysis and Visualization Division, Oak Ridge National Laboratory, Oak Ridge, Tennessee, 37831, USA, and [f]Tech-X Corporation, 8207 Main Street, Suite 3, Williamsville, New York, 14221, USA

1. One-dimensional Profile function

The functions are derived from the TOF profile function 1 in the GSAS program suite (Larson & Von Dreele, 2004) where ΔT is replaced by *Q*. To mostly reiterate the description in the GSAS manual, the profile function is the convolution of a Gaussian function

$$G\ Q\ = \frac{1}{\sqrt{2\pi\sigma^2}}\exp\ \frac{-\ Q-\mu\ ^2}{2\sigma^2}$$

with the exponential functions

$$E\ Q\ = 2Ne^{\alpha\ Q-\mu\ }\ \text{for (Q–μ) < 0}$$

and

$$E\ Q\ = 2Ne^{-\beta\ Q-\mu\ }\ \text{for (Q–μ) < 0}$$

where *N* is a scaling factor and μ is the mean of the Gaussian distribution. Then the convoluted function as given in the GSAS manual is

$$H\ Q\ = N\ e^{u}\ erfc\ y\ \ + e^{v}\ erfc\ z$$

where *erfc* is the complementary error function (available e.g. as scipy.special.erfc in Python) and

$$u = \frac{\alpha}{2}\ \alpha\sigma^2 - 2\ Q-\mu$$

$$v = \frac{\beta}{2}\ \beta\sigma^2 - 2\ Q-\mu$$

$$y = \frac{\alpha\sigma^2 + (Q-\mu)}{\sqrt{2\sigma^2}}$$

$$z = \frac{\beta\sigma^2 + (Q-\mu)}{\sqrt{2\sigma^2}}$$

For the case of the Gaussian with just one exponential, (Q–μ) < 0, the function is

$$H\ Q\ = Ne^{u}\ \text{erfc}\ y$$

and the least-squares refineable parameters are *N*, μ, σ and α plus the slope and constant for a linear background. For the convolution with two exponentials, the β parameter also needs to be refined.

Larson, A. C. & Von Dreele, R. B. (2004). General Structure Analysis System (GSAS), Los Alamos National Laboratory Report LAUR 86-748.

2. Tables for sapphire and natrolite crystal analyses

Table S1. Crystal data and structure refinement parameters for the sapphire crystal

Formula	Al_2O_3
Temperature, K	295 K
Crystal system	Trigonal
Space group	*R-3c*
a, Å	4.7521(1)
c, Å	12.9819(4)
V, Å^3	254.46(1)
Z	6
Size	1 mm diameter sphere
Radiation	Neutrons
Data collection technique	time-of-flight Laue
$\mu(\lambda)$, cm^{-1}	$0.369 + 0.006\lambda$
Max, min transmission	0.9708, 0.9768
d_{min}, Å	0.5
Refinement method	Full-matrix least-squares on *F*

Table S2. Crystal data and structure refinement parameters for the natrolite crystal

Formula	$Al_2H_4Na_2O_{12}Si_3$
Temperature, K	295 K
Crystal system	Orthorhombic
Space group	*Fdd*2
a, Å	18.3025(10)
b, Å	18.6544(10)
c, Å	6.5840(5)
V, Å^3	2247.9(2)
Z	8
Size	$1.25 \times 1.50 \times 1.75$ mm^3
Radiation	Neutrons
Data collection technique	time-of-flight Laue
$\mu(\lambda)$, cm^{-1}	$0.383, 0.143\lambda$
Max, min transmission	0.8909, 0.9496
d_{min}, Å	0.5
Refinement method	Full-matrix least-squares on *F*

3. Analyses of the BIPa neutron and x-ray data

Table S3. Crystal data and structure refinement parameters for the BIPa crystal

Formula	$C_{23}N_{11}O_{16}H_{25}$
Temperature, K	100(2) K
Crystal system	Monoclinic *C*
Space group	*C*2/*c*
a, Å	33.577
b, Å	7.661
c, Å	25.111
β, °	114.69
V, Å^3	5868.65
Z	8
Size	1.2 mm diameter sphere
Radiation	neutrons
Data collection technique	time-of-flight Laue
$\mu(\lambda)$, cm^{-1}	1.220 + 0.639λ
Max, min transmission	0.7474, 0.8873
d_{min}, Å	0.5
Refinement method	Full-matrix least-squares on *F*

Effects of varying integration radii of BIPa crystal; Spherical integration, Type 2

Based solely on maximizing the signal-to-noise ratio of the dataset the optimal integration radius was found to be 0.09 Å^{-1}. This method, however, does not indicate how sensitive the integration and subsequent structural refinement is with regards to larger or smaller integration radii and/or if systematic errors are introduced. To test this, the data were integrated using radii varying from 0.05 Å^{-1} to 0.11 Å^{-1} in steps of 0.01 Å^{-1}. Structural models were refined against the resulting intensities to allow a full comparison. The table below shows various refinement and model indicators to gauge the effect of the varying radii.

Table S4. Refinement and Model indicators of varying integration radii, Spherical integration, Type 2, for BIPa crystal.

Radius	*0.05*	*0.06*	*0.07*	*0.08*	*0.09*	*0.10*	*0.11*
Nref, Mantid	157186	157186	157186	157186	157186	157186	157186
Nref, Anvred	27693	29906	31555	32714	33611	34292	34941
Rejections in Refedt/ Rejections+I/σ(I)≥3σ	679/3363	531/4053	531/5315	649/6723	830/8240	1107/9732	1405/11283

GSAS:							
Nref	24330	25853	26240	25991	25371	24560	23645
RwF^2	0.143	0.113	0.090	0.080	0.080	0.087	0.099
RF^2	0.140	0.115	0.094	0.082	0.078	0.079	0.084
RwF	0.067	0.054	0.044	0.040	0.042	0.047	0.055
RF	0.081	0.066	0.056	0.051	0.049	0.051	0.056
<eds(d(C-C))>	0.00155	0.00121	0.00101	0.00094	0.00102	0.00119	0.00145
Hirshfeld rigid body test:							
Δ_{MSDA}	0.0005	0.0004	0.0003	0.0003	0.0003	0.0004	0.0004
$\Delta_{MSDA,rms}$	0.0007	0.0005	0.0004	0.0004	0.0004	0.0005	0.0006
$<\sigma(U)>$	0.0005	0.0004	0.0003	0.0003	0.0003	0.0004	0.0004
$\lvert\Delta_{MSDA,\ max}\rvert$	0.0015	0.0011	0.0009	0.0009	0.0012	0.0012	0.0012
Thermal parameters:							
$<\Delta U>$ ref: 3D, e010	0.002590(1857)	0.001483(1063)	0.000822(584)	0.000420(327)	0.000222(249)	0.000319(457)	0.000565(704)
$<U_{ii,X}/U_{ii,N}>$	0.813(83)	0.885(55)	0.936(33)	0.968(18)	0.989(10)	1.000(17)	1.006(32)
$<[\Delta U/\sigma(\Delta U)]^2>^{1/2}$	5.317	3.500	2.074	1.046	0.425	0.497	0.772
Thermal parameters:							
$<\Delta U>$ ref: X-ray	0.002690(1867)	0.001551(1034)	0.000898592)	0.000533(391)	0.000377(305)	0.000380(308)	0.000437(351)
$<U_{ii,X}/U_{ii,N}>$	0.768(59)	0.856(42)	0.917(31)	0.957(27)	0.982(29)	0.995(33)	1.001(41)
$<[\Delta U/\sigma(\Delta U)]^2>^{1/2}$	7.258	5.185	3.488	2.235	1.531	1.340	1.290

Increasing the radius from small values towards larger it is apparent that the number of reflections are increasing ($I/\sigma(I) \geq 1$). However, by rejecting outlier intensities based on the refined model ($0.1>F_o^2/F_c^2>10$, $|F_o^2-F_c^2|/\sigma(F_o^2)>10$) and rejecting intensities less than 3σ, it is apparent that the large radius integration does integrate more noise and the final set of data points in the refinement is lower than that of the intermediate radii.

The residuals show a minimum radius of 0.08 to 0.09 $Å^{-1}$, i.e. equivalent to the $I/\sigma(I)$ estimation. These radii also yield the smallest average uncertainty of the C-C bond distances indicating the highest precision.

The residuals only indicate the quality of the fit between the model and the data. To roughly compare the integrations it is important to compare the resulting models too. One of the most sensitive parts of the model with regards to systematic errors are the thermal parameters which can adapt to fit the error-prone data by refining to spurious values - even unphysical values in some cases. A simple test for internal consistency of the model is the Hirshfeld Rigid Body test (Hirshfeld, 1976) where the component of the thermal vibration towards bonded nearest neighbor atoms are compared. If the two atoms have nearly the same mass the difference between the vibration amplitudes towards each other should be small, i.e. a few times the estimated standard deviation. In the table it is seen that the various radii all lead to small and acceptable values, although the intermediate radii leads to values slightly lower than the extreme radii.

To compare the model to results from other integration methods and X-ray charge density models we have calculated the average difference between the U_{ij} values ($<\Delta U>$), the average ratio for the diagonal, U_{ii}, values ($<U_{ii,1}/U_{ii,2}>$) of the models and the RMS value of $\Delta U/\sigma(\Delta U)$ as suggested by Blessing (1995). The first section compares to the results using the 3D ellipsoidal integration (Type 3), and the second to the charge density model refined against X-ray data collected at 100 K.

The smallest values of $<\Delta U>$ are found for a radius of 0.09 $Å^{-1}$ with values increasing rapidly when using smaller radii. A similar effect can be seen for the $<U_{ii,1}/U_{ii,2}>$ which deviates strongly from unity at small radii.

Based on the discussion above it is clear that the 0.09 $Å^{-1}$ integration radius both lead to a good fit and a physically sound model that agrees exceptionally well with X-ray data. It is however unclear how the systematic errors are introduced. We have plotted the intensity ratio between 0.09 $Å^{-1}$ and the other models as a function of d-spacing in figure S1.

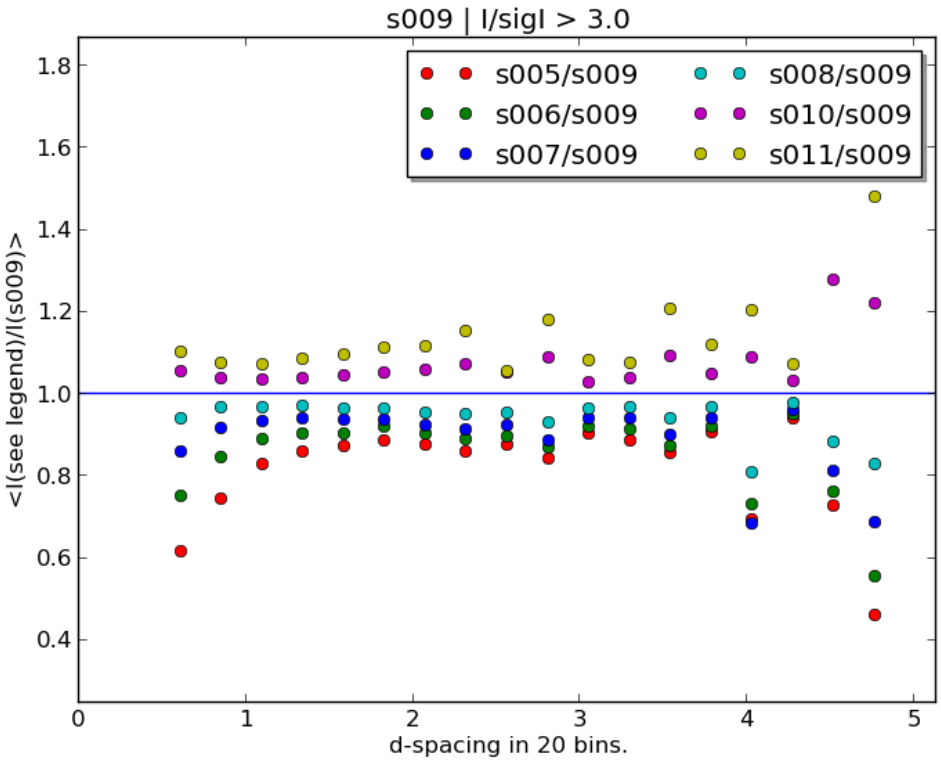

Figure S1: The ratio between intensities obtained with varying radii and intensities obtained using r = 0.09 $Å^{-1}$ for BIPa crystal. Only reflections included in the model refinement are included. The notation s0XX refers to spherical integration with r = 0.XX $Å^{-1}$.

It is clear that, as expected, similar radii do lead to similar results. The two high d-spacing points are based on only one reflection per point. For the smaller radii the intensities at both high and low d-spacings are underestimated. At high d-spacings the crystal

mosaicity and beam divergence leads to more diffuse peaks. At small d-spacings the intensities are stronger which leads to longer tails around the reflections. For radii larger than 0.09 $Å^{-1}$ there is a deviation at high d-spacing, i.e. a larger radii leads to a larger intensity (and larger $I/\sigma(I)$) indicating too small of a radius for these (two) reflections.

Despite potentially loosing intensity for the high d-spacing reflections the overall refinement and comparison with X-ray data seems to be better for the integration using a 0.09 $Å^{-1}$ radius.

Effects of varying integration radii for BIPa crystal; 1D integration, Type 4
The same radii (0.05 to 0.11 $Å^{-1}$ in 0.01 $Å^{-1}$ increments) were used and the same rejection criteria etc. were used.

Table S5. Refinement and Model indicators of varying integration radii, Cylindrical integration, Type 4.

Radius	*0.05*	*0.06*	*0.07*	*0.08*	*0.09*	*0.10*	*0.11*
Nref, Mantid	157186	157186	157186	157186	157186	157186	157186
Nref fitted	35493	36149	36127	35933	35608	34956	34566
Nref, Anvred	23241	23545	23440	23271	22962	22570	22217
Rejections in Refedt/ Rejections+$I/\sigma(I)\geq 3\sigma$	172/1592	142/1691	131/1743	131/1877	110/2009	139/2082	148/2239
GSAS:							
Nref	21649	21854	21697	21394	20953	20488	19078
RwF^2	0.084	0.074	0.072	0.072	0.073	0.075	0.076
RF^2	0.079	0.071	0.070	0.070	0.072	0.075	0.076
RwF	0.041	0.037	0.036	0.037	0.038	0.039	0.040
RF	0.046	0.043	0.043	0.043	0.044	0.046	0.047
<eds(d(C-C))>	0.00104	0.00094	0.00094	0.00097	0.00103	0.00111	0.00115
Hirshfeld rigid body test:							
Δ_{MSDA}	0.0003	0.0003	0.0003	0.0003	0.0004	0.0003	0.0004
$\Delta_{MSDA,rms}$	0.0004	0.0004	0.0004	0.0004	0.0005	0.0005	0.0005
$<\sigma(U)>$	0.0003	0.0003	0.0003	0.0003	0.0003	0.0003	0.0003
$\lvert\Delta_{MSDA,\ max}\rvert$	0.0007	0.0007	0.0009	0.0009	0.0015	0.0014	0.0010
Thermal parameters:							
$<\Delta U>$ ref: 3D, e010	0.001030(744)	0.000440(448)	0.000422(413)	0.000620(503)	0.000776(620)	0.000894(708)	0.000998(727)
$<U_{ii,X}/U_{ii,N}>$	0.922(42)	0.980(24)	1.018(24)	1.045(31)	1.064(39)	1.079(47)	1.091(55)
$<[\Delta U/\sigma(\Delta U)]^2>^{1/2}$	2.514	0.906	0.862	1.392	1.791	2.059	2.267
Thermal parameters:							
$<\Delta U>$ ref: X-ray	0.001074(700)	0.000420(332)	0.000340(270)	0.000475)377)	0.000613(484)	0.000744(567)	0.000848(647)
$<U_{ii,X}/U_{ii,N}>$	0.899(35)	0.971(29)	1.018(34)	1.050(40)	1.073(49)	1.093(57)	1.109(63)
$<[\Delta U/\sigma(\Delta U)]^2>^{1/2}$	3.987	1.823	1.405	1.918	2.392	2.702	2.967

The picture is pretty much the same as seen for the spherical integration with a few exceptions; the most obvious being the optimal radius seem to be 0.07 $Å^{-1}$, i.e. smaller than the one found for the spherical integration. The smaller radius is due to the peak shapes obtained at TOPAZ, which extends more along the hkl-vector (TOF direction) than the two perpendicular directions. The integration sphere has to account for this while it is intrinsically accounted for in the cylindrical integration.

The number of intensities obtained by this method is significantly smaller than the number obtained using the spherical integration (and ellipsoidal integration), which is due to the fact that spurious reflections are rejected at an early step. The number of intense peaks ($I/sig(I) \geq 5$) are similar, i.e. the fitting of the 1D profiles misses some of the low intensity reflections. We are currently working on a better approach where the weaker peaks are constrained to the profile function of the more intense peaks in the same region of space and TOF. The lower number of reflections leads to artificially lower residual values when comparing the values to the other methods.

Nearly all the values tabulated indicate that 0.06 to 0.07 $Å^{-1}$ is the optimal radius. The agreement of the thermal parameters with the charge density model is excellent, even slightly better than that found for the spherical integration.

As for the spherical integration method we have plotted the intensity ratio between the various radii and the optimal value of 0.07 $Å^{-1}$. In contrast to the spherical integration where deviations from unity were found at both high and low d-spacings the cylindrical integration only shows a deviation at small d-spacings. As high d-spacings the extra length of the cylinder picks up the tails not integrated using the spherical method. The deviations at low d-spacings indicate that the cylinder radii may be too small, at large Q. However, the overall model seems to be the best at the 0.07 $Å^{-1}$ radius. We are currently working on implementing an algorithm to vary the radii based on the absolute length of the Q-vector.

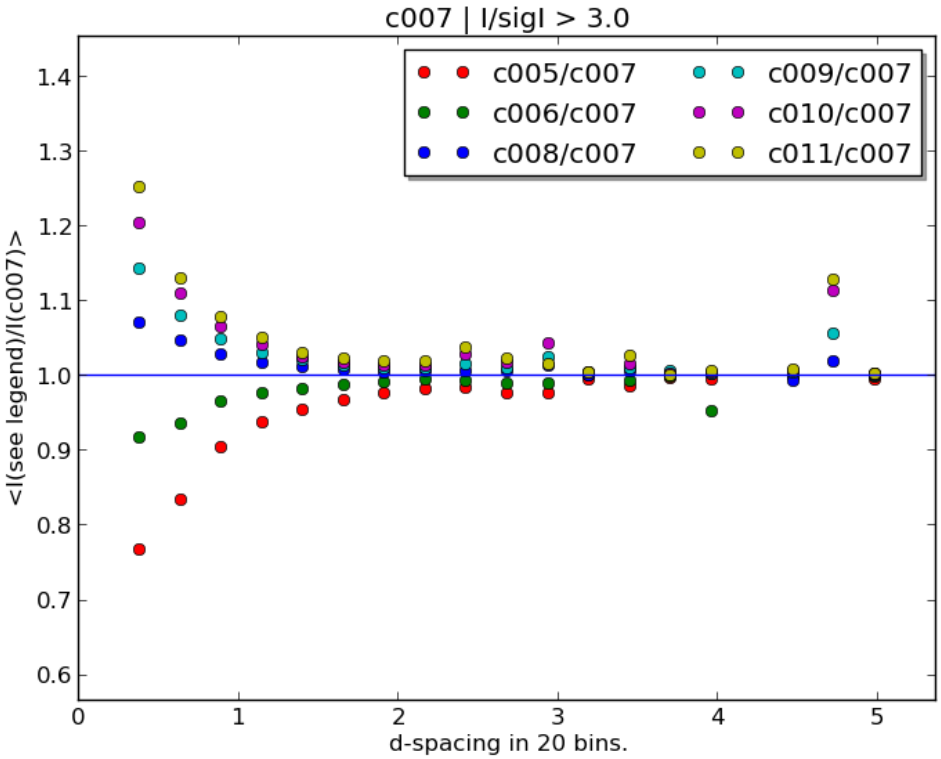

Figure S2: The ratio between intensities obtained with varying radii and intensities obtained using r = 0.07 $Å^{-1}$. Only reflections included in the model refinement are included. The point at approx. 4.75 Å is due to one reflection only. The notation c0XX refers to cylindrical integration r = 0.XX $Å^{-1}$.

Ellipsoidal integration, Type 3

As described it is possible to either refine all three components of the ellipsoid or fix the major axis to a user specified value. Table S6 shows refinement results for integrations with the major axis fixed and freely refined.

Table S6. Refinement and Model indicators of varying integration radii, Ellipsoidal integration, Type 3, for BIPa crystal.

Major axis length	*0.05*	*0.06*	*0.07*	*0.08*	*0.09*	*0.10*	*0.11*	*Refined*
Nref, Mantid	157186	157186	157186	157186	157186	157186	157186	157186
Nref, Anvred	26826	29084	30815	32089	33077	33651	34424	37908
Rejections in Refedt/ Rejections+I/σ(I)≥3σ GSAS:	804/2860	590/3033	539/3713	607/4822	720/6350	878/7765	1177/9364	2574/13882
Nref	23966	26051	27102	27267	26727	25886	25060	24026
RwF^2	0.155	0.127	0.102	0.085	0.077	0.078	0.084	0.109
RF^2	0.146	0.123	0.103	0.089	0.080	0.078	0.080	0.098
RwF	0.073	0.060	0.049	0.042	0.039	0.040	0.045	0.061

RF	0.086	0.072	0.061	0.054	0.051	0.051	0.053	0.067
<eds(d(C-C))>	0.00168	0.00131	0.00105	0.00092	0.00090	0.00095	0.00111	0.00159
Hirshfeld rigid body test:								
Δ_{MSDA}	0.0006	0.0004	0.0003	0.0003	0.0003	0.0003	0.0004	0.0006
$\Delta_{MSDA,rms}$	0.0008	0.0005	0.0004	0.0003	0.0003	0.0004	0.0005	0.0007
$<\sigma(U)>$	0.0005	0.0004	0.0003	0.0003	0.0003	0.0003	0.0003	0.0005
$\lvert\Delta_{MSDA,\ max}\rvert$	0.0019	0.0010	0.0010	0.0008	0.0008	0.0010	0.0011	0.0016
Thermal parameters:								
$<\Delta U>$ ref: 3D, e010	0.003160(2230)	0.001877(1334)	0.001084(763)	0.000607(443)	0.000283(233)	0.000000	0.000268(316)	0.000733(894)
$<U_{ii,X}/U_{ii,N}>$	0.782(93)	0.859(66)	0.916(42)	0.955(25)	0.983(14)	1.000	1.008(16)	1.011(41)
$<[\Delta U/\sigma(\Delta U)]^2>^{1/2}$	6.055	4.271	2.709	1.520	0.661	0.000	0.473	0.931
Thermal parameters:								
$<\Delta U>$ ref: X-ray	0.003262(2269)	0.001944(1303)	0.001148(753)	0.000675(464)	0.000397(327)	0.000332(283)	0.000350(282)	0.000512(427)
$<U_{ii,X}/U_{ii,N}>$	0.732(65)	0.824(49)	0.893(35)	0.941(28)	0.974(27)	0.995(31)	1.005(34)	1.007(47)
$<[\Delta U/\sigma(\Delta U)]^2>^{1/2}$	8.120	6.127	4.313	2.851	1.820	1.417	1.306	1.365

It is clear that the freely refined ellipsoids do not lead to a good fit between data and model with residual values much higher than principle axis fixed at 0.09 to 0.10 $Å^{-1}$. Surprisingly the comparison of the thermal parameters from this refinement and that of the charge density model shows a reasonable agreement, although not a good as the refinements against data integrated with fixed principle axis length around 0.10 $Å^{-1}$.

Varying the principle axis length show that the best value, based on residual values, is 0.09 $Å^{-1}$ while 0.10 lead slightly higher residuals. However, comparing thermal parameters to the charge density model, the 0.10 $Å^{-1}$ model has slightly better merits and is thus chosen to be the best radii. The differences between the two are minor and both show a good fit to the data and excellent agreement with the charge density model.

By comparing the intensities obtained for the various axis lengths to the best length, 0.10 $Å^{-1}$, it can be seen that the main differences occur at low d-spacings and mainly for the small axis lengths. It can also be seen that the intensities freely refined ellipsoids vary quite significantly.

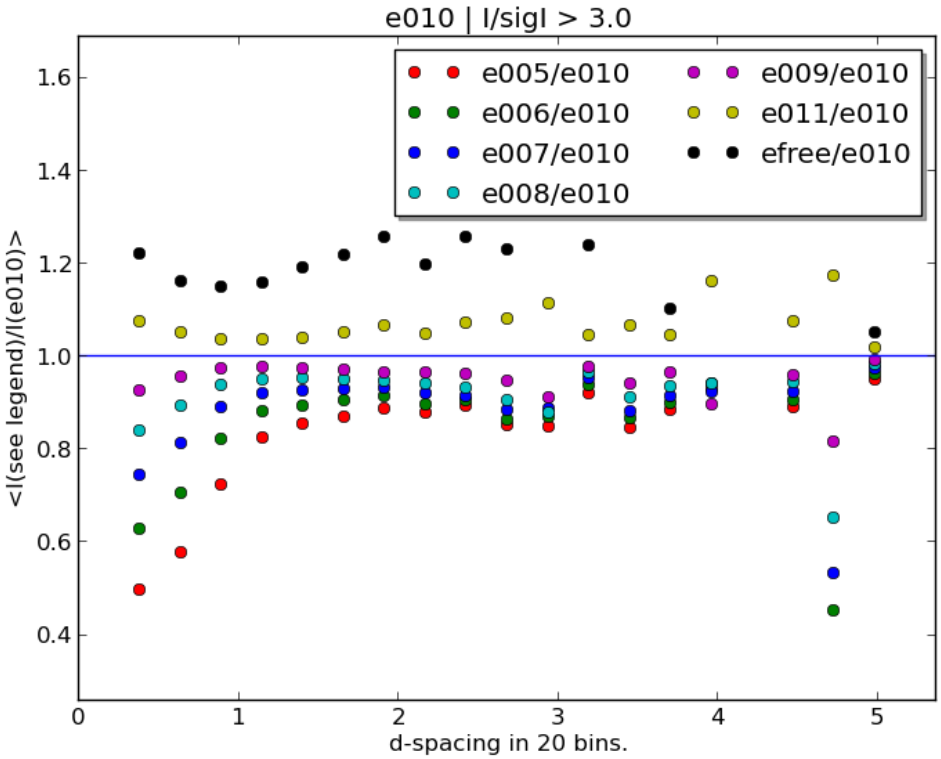

Figure S3: The ratio between intensities obtained with varying principle axis length and intensities obtained using a length of 0.10 $Å^{-1}$. Only reflections included in the model refinement are included. The point at approx. 4.75 Å is due to one reflection only. The notation e0XX refers to the principle axis length as 0.XX $Å^{-1}$. 'efree' refers to freely refined axis.

4. BIPa; X-ray data collection and charge density refinement.

A yellow block shaped crystal with dimensions of 160 x 200 x 290 μm3 was mounted on a thin glass fiber using epoxy resin on the end of a standard goniometer head. The assembly was mounted on an Oxford Diffraction (now Agilent Technologies UK Ltd.) SuperNova system at the Department of Chemistry, Aarhus University, Denmark. The sample was flash cooled to 100 (2) K using a liquid N2 cryostream from Oxford Cryosystems. Data was collected using 1° wide ω-scans. A total of 162776 (41957 unique, 98.4% completeness) reflections up to a maximum resolution of 1.2 $Å^{-1}$ were integrated using the program CrysAlisPro (Agilent Technologies UK Ltd., 2010). Equivalent reflections were merged in SORTAV(Blessing, 1997) yielding an R_{int} value of 3.81%. 27262 reflections with 3 or more independent measurements and a max resolution of 1.1 $Å^{-1}$ were used in the refinement.

The structure was refined in SHELXL-97 (Sheldrick, 2008) using the reported structure by Overgaard *et al*. (Overgaard *et al*., 1999) This model was imported into the XD2006 (Volkov *et al*., 2006) program suite. Coordinates and thermal parameters of the heavy atoms were refined against the high order reflections (> 0.80 $Å^{-1}$)to get unbiased positions. In the subsequent refinements cycles the multipoles were gradually added and refined against all data. For all heavy atoms all symmetry allowed poles up to octupoles were included. For hydrogen a monopole and a bond directed dipole were refined. Separate κ and κ' parameters were refined for C, O and N. All parameters were co-refined until convergence.

formula	$C_{25}N_{11}O_{16}H_{25}$
M (g mol^{-1})	711.51
crystal system	Monoclinic
space group	C2/2
T (K)	100(2)
sample size (μm)	160 x 200 x 290
a (Å)	33.5939(5)
b (Å)	7.6658(1)
c (Å)	25.1324(3)
β (˚)	114.716(2)
V ($Å^3$)	5879.3(1)
λ (Å)	0.71073
Z	8
μ (mm^{-1})	0.077
T_{min}/T_{max}	0.990/0.985
unique reflections: all / $N_{meas} \geq 3$, $\sin\theta/\lambda \leq 1.1$ $Å^{-1}$	41957 / 27262
completeness	98.4 %
<N>	3.9
R_{int}	3.81%
N_{par}	1306

N_{obs}	21277
R(F), R(F^2)	3.02%, 2.96%
R_w(F), R_w(F^2)	4.25%, 7.21%
Goodness-of-fit	0.8741
Min, Max residual density (e $Å^{-3}$): $\sin\theta/\lambda \leq 1.1$ $Å^{-1}$ / $\sin\theta/\lambda \leq 0.8$ $Å^{-1}$	-0.26, 0.31 / -0.16, 0.17

Agilent Technologies UK Ltd. (2010). CrysAlisPro. Version 171.34.44.

Blessing, R. H. (1997). J. Appl. Crystallogr. 30, 421-426.

Overgaard, J., Schiott, B., Larsen, F. K., Schultz, A. J., MacDonald, J. C. & Iversen, B. B. (1999). Angew Chem Int Edit 38, 1239-1242.

Sheldrick, G. M. (2008). Acta Crystallogr., Sect. A: Found. Crystallogr. 64, 112-122.

Volkov, A., Macchi, P., Farrugia, L. J., Gatti, C., Mallinson, P., Richter, T. & Koritsanszky, T. (2006). XD2006. Rev. 5.34. University at Buffalo, State University of New York, NY, USA, University of Milano, Italy, University of Glasgow, UK, CNR-ISTM, Milano, Italy, and Middle Tennessee State University, TN, USA.

5. TOPAZ instrument resolution

Equation (8) in Schultz et al. (2005) is given as:

$$\Delta t_{pulse}\ \ FW\ \ \leq 505L\ \ d_{min}^{2}\ \ a\ \ \sin\theta$$

where $\Delta t_{pulse}\ \ FW\ \ $ is the full width of the neutron pulse for the wavelength associated with $d_{\min}$ and the theta angle. This equation is derived from Jauch (1997) who gives the equation for the FWHM pulse width. This equation was solved for a with $d_{\min}$ = 0.5 Å, θ = 45 deg, and Δt = 23 microseconds. The latter value was extrapolated from Table 4 in Schultz et al. (2005), and then multiplied by 1.5 to be conservative about the resolution predictions.

Jauch, W. (1997). *J. Neutron Research*. **6**, 161–171.

Schultz, A. J., Thiyagarajan, P., Hodges, J. P., Rehm, C., Myles, D. A. A., Langan, P., & Mesecar, A. D. (2005). *J. Appl. Cryst.* **38**, 964–974.